Proc. Natl. Acad. Sci. USA
Vol. 77, No. 8, pp. 4524–4528, August 1980
Biochemistry

Molecular dissection of Rauscher virus gp70 by using monoclonal antibodies: Localization of acquired sequences of related envelope gene recombinants

[murine retroviruses/xenotropic parent/hybridomas/peptide patterns (fingerprinting)/mink cell focus-inducing viruses]

HENRY L. NIMAN AND JOHN H. ELDER

Department of Cellular and Developmental Immunology, Research Institute of Scripps Clinic, La Jolla, California 92037

Communicated by Frank J. Dixon, May 1, 1980

ABSTRACT **Using hybridoma-specific immune precipitations of fragments derived from Rauscher virus gp70, coupled with peptide patterns (fingerprinting) and partial amino acid sequence analyses, we have generated a linear map of Rauscher gp70. We used a panel of 56 hybridomas derived from the fusion of the drug-selected SP-2 myeloma line with spleen cells from either a 129 GIX$^+$ or a GIX$^-$ mouse immunized with purified Rauscher virus gp70. The results showed that by "natural" breakdown, gp70 splits into predominant fragments with M_r 45,000 (P45), 34,000 (P34), and 32,000 (P32). Peptide fingerprinting of these as well as overlapping fragments coupled with partial amino acid sequence analyses allowed us to align the fragments into the linear arrangement NH_2-P45-P32-COOH, with P34 being an NH_2-terminal degradation product of P45. Of the 56 hybridomas, 20 immunoprecipitated both P45 and P34; 18 immunoprecipitated only P45; and 18 immunoprecipitated only P32. The hybridomas thus define three domains of the molecule as NH_2-P45/P34, P45 only, and P32-COOH. Allowing these hybridomas to react with two Rauscher-derived envelope gene recombinant viruses yielded the following results: (*i*) all 20 P45/34 reactors bound to the two Rauscher recombinants; (*ii*) of 18 P45-only hybridomas, 10 reacted; and (*iii*) only 1 of 18 P32 reactors bound to the Rauscher recombinants. This last hybridoma reacted with various murine retroviruses, indicating that it was directed at conserved determinants of gp70. Peptide fingerprinting of R-gp70, the recombinant gp70s, and their respective breakdown products confirmed the homologies and nonhomologies defined by the hybridomas. Furthermore, peptide patterns showed that these acquired sequences on the COOH-terminal portion of the recombinant gp70s are related to xenotropic virus gp70s.**

Recent evidence suggests that recombination within the major envelope glycoprotein, gp70, of many retroviruses is involved in generating highly leukemogenic (murine leukemia viruses (MuLVs) (1–13). Although the parents of the recombinant mink cell focus-inducing viruses of each system are quite distinct, the site of recombination appears to be confined to a discrete region of the envelope gene. The present study focuses on the structure of Rauscher MuLV (R-MuLV) gp70, which we have used to establish a framework upon which to compare other gp70s of interest. We have prepared monospecific hybridomas directed against R-MuLV gp70 and have utilized these antibodies coupled with specific cleavage fragments and partial sequence data to order the peptides within the molecule. By deriving similar fragments from gp70s of recombinant viruses derived from R-MuLV and comparing peptide structures of these fragments, we have been able to determine that the primary change in the recombinants begins approximately 30,000 daltons from the NH_2 terminus and extends through the COOH-terminal portion of the molecule. Peptide analyses indicate that the substituted region in the mink cell focus-inducing viruses gp70 shares peptides common to endogenous xenotropic viruses.

The publication costs of this article were defrayed in part by page charge payment. This article must therefore be hereby marked "*advertisement*" in accordance with 18 U. S. C. §1734 solely to indicate this fact.

MATERIALS AND METHODS

Viruses. R-MuLV was kindly provided by Jack Gruber (Resources Branch, National Cancer Institute). All other viruses used in this study were produced in either mouse SC-1 cells or mink lung CCL64 cells, isolated and purified as described (2, 14).

Gp70 Isolation and Peptide Fingerprinting. Gp70 was purified from Nonidet P-40-disrupted R-MuLV by phosphocellulose (Whatman P11) chromatography (15), or by immunoaffinity chromatography (2, 14) and subjected to Na-DodSO_4/polyacrylamide gel electrophoresis (16). Bands corresponding to gp70 or specific breakdown products were sliced from the gel and subjected to tryptic and chymotryptic digestion and two-dimensional separation of the peptides as described (2, 14).

Peptide Fragments. Fragments were primarily generated by the "natural" breakdown of unpurified gp70. Viruses were disrupted with Nonidet P-40 and radiolabeled with ^{125}I (17 mCi/mmol; 1 Ci = 3.7×10^{10} becquerels; ICN) as described (2, 14). The virus was then dialyzed against phosphate-buffered saline for 16 hr at 25°C. Additional fragments were produced from limited digestion with V8 protease (50 μg/ml in 0.4% NH_4HCO_3) by addition of 5 μl of enzyme solution to 100 μl of buffer containing 8×10^6 cpm of ^{125}I-labeled gp70 (^{125}I-gp70) and incubation at 37°C for 30 min. The reaction was terminated by immersion of the samples in boiling H_2O for 2 min. Fragments were also derived by treatment of gp70 with 88% formic acid for 4 hr at 60°C; this reaction was terminated by lyophilization.

Immunizations and Fusions. Either 129 GIX$^+$ or 129 GIX$^-$ mice were immunized subcutaneously or intraperitoneally with 50 μg of R-MuLV gp70 in complete Freund's adjuvant. Two weeks later, 50 μg of gp70 in alum (10 mg/ml) was injected interperitoneally. An additional injection with 50 μg of gp70 was given intravenously 2 months later. Five days after the final injection, nucleated spleen cells were fused with 2×10^7 SP-2 drug-marked nonimmunoglobulin-secreting myeloma cells (17) as described (18). The cells were then resuspended in 0.1 mM hypoxanthine/1 μM methotrexate/32 μM thymidine in minimal essential medium supplemented with 10% fetal calf serum. Cells were plated into 16 microtiter plates (96-well, Falcon). Macroscopic colonies were transferred to 24-well Linbro plates and assayed 4–8 days later.

Antibody Binding Assay. Anti-gp70 antibodies were detected by a binding assay (19) with ^{125}I-labeled affinity-purified

Abbreviations: MuLV, murine leukemia virus; R-MuLV Rauscher MuLV.

goat anti-rabbit antibody kindly provided by N. Klinman of this institute. Rabbit anti-mouse antiserum supplemented with rabbit anti-mouse IgE was generously provided by D. Katz of this institute. Virus-coated flexible microtiter plates were prepared (20) and assayed as described (19).

By using affinity-purified goat anti-rabbit antibody conjugated with glucose oxidase (21), the isotype of each hybridoma was determined by substituting absorbed rabbit anti-mouse isotype antibodies (generously provided by J. Teale, this Institute) for the broadly reactive anti-mouse immunoglobulin anti-sera in the above procedure.

Immune Precipitation. Radiolabeled virus ($1–2 \times 10^6$ cpm) was incubated with 50 μl of tissue culture supernatant (adjusted to 0.5% Nonidet P-40) for 30 min at 37°C and overnight at 4°C. The mixture was then incubated for 30 min at 37°C with 20 μl of a 1:10 dilution of rabbit anti-mouse κ and λ light chain antisera (Miles) to facilitate precipitation by Pansorbin of nonbinding isotypes. Pansorbin (50 μl) was added and the bound immunoglobulin was washed twice with 500 mM LiCl/10 mM Tris·HCl, pH 8.5 (22). The resulting pellet was heated at 100°C for 2 min in 100 μl of 0.5% 2-mercaptoethanol/1% NaDodSO$_4$/20% (vol/vol) glycerol and subjected to electrophoresis as above.

RESULTS

Characterization of gp70 Fragments. More than 3000 hybridomas were generated in this study, of which 300 had binding activity for R-MuLV and more than 100 were stable. Based upon reactivity patterns generated by binding assays with other viruses, immunoprecipitation of gp70 fragments, and immunofluorescence of virus-infected cells, more than 30 determinants were defined by the 56 hybridomas used in this study (unpublished data). The 56 hybridomas used in this study were selected for their ability to immunoprecipitate "natural" breakdown products of gp70. gp70 has been shown to break down to two major products of apparent M_rs of approximately 45,000 and 32,000 (23). Because monoclonal antibodies react with a single antigenic determinant, they should only immunoprecipitate antigenically related polypeptides. Fig. 1 shows immunoprecipitation of ^{125}I-labeled R-MuLV with a goat antiserum against R-MuLV gp70 as well as tissue culture supernatants of three hybridomas. Major polypeptides of M_r 70,000 (gp70), 45,000 (P45), 34,000 (P34), and 32,000 (P32) all were precipitated by the broadly reactive goat antiserum.

Fig. 2 shows the chymotryptic peptides of the indicated bands of Fig. 1 precipitated by each specific hybridoma. gp70 was degraded via two parallel pathways. P45 was clearly related to P34 and differed primarily in the loss of two major peptides. One of these peptides (left arrow in *B*) comigrated with a peptide present in P34 and its loss was indicated by a depletion in that region of the P45 map relative to the map of P34. P32 was distinct from P45 and contained the gp70 peptides not present in P45. The peptide map of the minor P42 component was essentially the same as P32 (data not shown) and possibly ran at a higher apparent M_r due to the presence of a full complement of glycosidic sidechains or to residual association with P15E. By mass, P32 is the most predominant form in which this portion of the gp70 is represented. An overlap fragment generated by cleavage with V8 protease contained peptides of P32 as well as two peptides that comigrated with the two P45-specific peptides. Note that all the major peptides of gp70 are accounted for by the addition of P45 and P32 and that P45 and P32 are totally distinct from one another.

Orienting the Peptides. P45 and P32 were oriented with gp70 by NH_2-terminal sequence analysis. Because R-MuLV gp70 has a tyrosine at position 11 (ref. 24, and our unpublished data), we were able to determine the sequence of ^{125}I-labeled R-MuLV gp70, P45, and P32 for 14 residues and to learn that P45 also has a tyrosine at position 11 whereas P32 has tyrosine

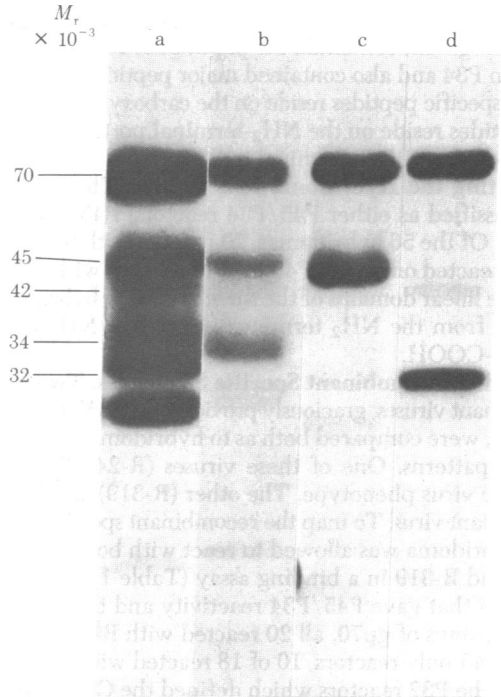

FIG. 1. Immunoprecipitations on NaDodSO$_4$/polyacrylamide gel electrophoresis of R-MuLV gp70 and its natural breakdown products. ^{125}I-Labeled gp70 was treated as described in *Materials and Methods* and incubated with either a broadly reactive goat (G230) anti-gp70 serum (lane a) or monospecific hybridoma supernatants (anti-45/34, lane b; anti-45, lane c; anti-32, lane d). Hybridoma R$_1$01D09-02 (Table 1) was used to precipitate P45 and P34 (anti-45/34); hybridoma R$_1$06B08-01-02 precipitated only P45 (anti-45); and R$_2$09E11-01-03 precipitated P32 and a minor component of M_r 42,000 (anti-32). The figure is a composite of different gel runs and thus some discrepancy in mobility of nonspecific fast-migrating components is apparent, but it is not significant.

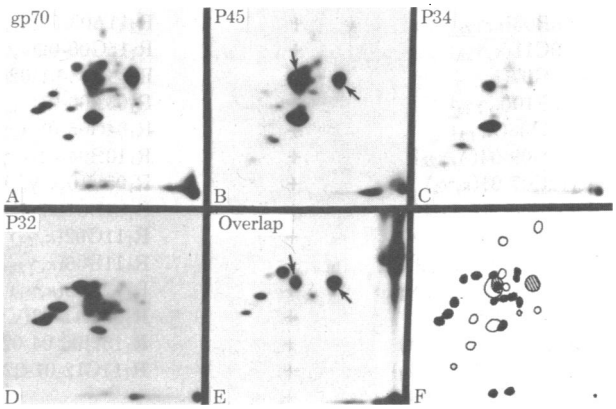

FIG. 2. Two-dimensional separation of chymotryptic peptides of R-MuLV gp70 and natural breakdown products. (*A*) Total R-MuLV gp70; (*B*) P45 immunoprecipitated by antibodies of R$_2$06B08-01-02 (see Table 1); (*C*) P34 immunoprecipitated by R$_1$01C09-01; (*D*) P32 immunoprecipitated by R$_2$09C11-02; (*E*) M_r 55,000 fragment generated by V8 protease; (*F*) composite drawing of gp70 peptides indicating relative contribution of the various fragments. Closed circles, derived from P32; open circles, shared by P45 and P34; crosshatched circles, lost from P45 (arrows in *B*) in transition to P34 (*C*) and present in the V8 overlap fragment (arrows in *E*).

at positions 4 and 10 (data not shown). The protease V8-derived overlap fragment contained the peptides of P45 that were absent from P34 and also contained major peptides of P32. Thus, the P45-specific peptides reside on the carboxyl end of P45; the P34 peptides reside on the NH_2-terminal portion of P45; and P32 is located COOH-terminal to P45.

Orienting the Hybridoma Reactivities. The hybridomas were classified as either P45/P34 reactors, P45-only, or P32 reactors. Of the 56 hybridomas, 20 reacted with both P45 and P34, 18 reacted only with P45, and 18 reacted with P32 (P42). Thus, the linear domains of the three groups of hybridomas are oriented from the NH_2 terminus of gp70 as NH_2-P45/P34-P45-P32-COOH.

Mapping Recombinant Specific Sequences. Two R-MuLV recombinant viruses, graciously provided by M. Vogt of the Salk Institute, were compared both as to hybridoma reactivity and peptide patterns. One of these viruses (R-240) has an XC^- ecotropic virus phenotype. The other (R-319) is a dual tropic recombinant virus. To map the recombinant specific sequences, each hybridoma was allowed to react with both recombinant R-240 and R-319 in a binding assay (Table 1). Of the 20 hybridomas that gave P45/P34 reactivity and thus defined the NH_2 terminus of gp70, all 20 reacted with R-240 and R-319. Of the P45-only reactors, 10 of 18 reacted with R-240 and R-319. Of the P32 reactors which defined the COOH terminus, only one reacted with R-240 and R-319. This latter hybridoma also reacted with primate and feline viruses and thus is specific for interspecies determinants that reside in P32.

Fig. 3 compares the peptide relatedness between R-MuLV gp70 and the recombinant R-319 gp70. The peptides shared between R-MuLV gp70 and R-319 gp70 (open circles, Fig. 3*C*) are the major peptides of P45/P34 (compare to Fig. 2*F*) with the exception of a doublet of peptides (upper left, Fig. 3*C*) which are common to all gp70s and reside in the COOH-terminal P32 fragment (Fig. 2*D*). Comigrations indicate that one of the P45-specific peptides (defined in Fig. 2) is shifted upward in mobility in R-319 gp70 (arrow within peptide, Fig. 3*C*).

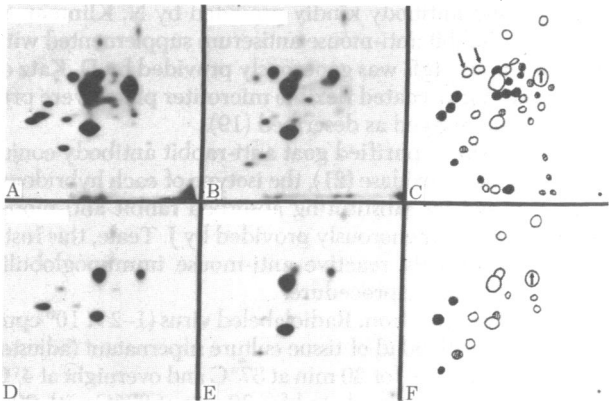

FIG. 3. Two-dimensional separation of chymotryptic peptides of R-MuLV gp70, R-MuLV-derived recombinant R-319 gp70, and formic acid-generated breakdown fragments. (*A*) Total R-MuLV gp70. (*B*) Total R-319 gp70. (*C*) Composite of *A* and *B*, demonstrating the extent of change. Closed circles, R-MuLV-specific peptides; open circles, common peptides; crosshatched circles, peptides found only in R-319 gp70; arrows, peptides common to all gp70s including those of primate and feline retroviruses; arrow within circle, peptide moves slightly faster (shifts up) in R-319 gp70 relative to R-MuLV gp70. Note that two dominant peptides of natural breakdown P32 (Fig. 2 *D* and *F*) are in R-FA45 (*D*), establishing their NH_2-terminal location on P32. Additionally, note that R-319 FA45 (*E*) lacks these peptides and thus this region of the molecule represents a major region of difference between R-MuLV gp70 and R-319 gp70.

Table 1. Peptide fragment and recombinant virus reactivities of anti-R-MuLV Gp70 hybridomas

P45/34 reactors*	Recombinant reactivity†	P45-only reactors‡	Recombinant reactivity†	P32 reactors§	Recombinant reactivity†
R_1O4C10(κ,γ_1)	+	$R_1$01G11(κ,γ_1)	+	$R_1$16G07(κ,γ_{2a})	−
$R_1$12G05(κ,γ_{2a})	+	$R_1$10G02(κ,γ_{2a})	+	$R_1$10B06(κ,γ_1)	−
$R_1$11B04(κ,γ_{2a})	+	$R_1$01D11(κ,γ_{2a})	+	$R_2$11D10(κ,γ_1)	−
$R_1$08H04(κ,γ_1)	+	$R_1$02F10(κ,γ_1)	+	$R_2$01F01(κ,γ_{2a})	−
$R_1$06B03(κ,γ_{2a})	+	$R_2$11A03-04(κ,γ_1)	+	$R_2$01C08(κ,γ_1)	−
$R_1$09C11(κ,γ_{2a})	+	$R_1$15G05-02(κ,γ_{2a})	+	$R_2$14D01(κ,γ_1)	−
$R_2$13G07(λ,γ_1)	+	$R_2$06B08-01-02(κ,γ_{2a})	+	$R_1$13H03(κ,γ_1)	−
$R_1$12F10(κ,γ_{2a})	+	$R_1$05A06-01(κ,γ_{2a})	+	$R_1$09C12(λ,γ_{2a})	+
$R_1$12H06(λ,γ_1)	+	$R_1$04G05-01(κ,γ_{2b})	+	$R_1$15C06(κ,γ_1)	−
$R_1$02G09-04(λ,γ_{2a})	+	$R_1$10B04-01(κ,γ_1)	+	$R_1$15D04(κ,γ_1)	−
$R_1$12C07-01(κ,γ_1)	+	$R_1$05E10(κ,γ_{2a})	−	$R_1$13A11-02(κ,γ_1)	−
$R_1$08E03-01(κ,γ_1)	+	$R_1$01B01(κ,γ_1)	−	$R_2$09C11-02(κ,γ_{2b})	−
$R_1$01D09-01(κ,γ_{2b})	+	$R_1$11G02(κ,γ_1)	−	$R_2$03D11-03(κ,γ_1)	−
$R_2$03F09-02(κ,γ_{2b})	+	$R_1$11B06(κ,γ_{2b})	−	$R_1$04D05-02(κ,γ_1)	−
$R_2$10G05-08-03(κ,γ_1)	+	$R_1$12C02(κ,γ_1)	−	$R_1$04C07-01(κ,γ_{2b})	−
$R_1$01C12-04(κ,γ_{2a})	+	$R_1$01H11-03(κ,γ_1)	−	$R_1$11E10-01(κ,γ_1)	−
$R_1$10D05-07-02(κ,α)	+	$R_1$15H06-04-02(κ,γ_1)	−	$R_2$09E11-01-03(κ,γ_1)	−
$R_1$16C12-01-02(κ,γ_3)	+	$R_1$11C12-01-02(κ,γ_1)	−	$R_1$16D02-04-01-02(κ,ε)	−
$R_1$05E06-05-01(κ,γ_1)	+				
$R_1$06F09-02(κ,γ_{2b})	+				

Hybridoma with subscript 1 originated from hyperimmune spleen cells of a 129 G_{IX}^- mouse. Subscript 2 hybridomas came from 129 G_{IX}^+ hyperimmune spleen cells. The symbols in parentheses refer to isotype of light and heavy chains, respectively. Abbreviations are: α, IgA; γ_1, IgG_1; γ_{2a}, IgG_{2a}; γ_{2b}, IgG_{2b}; γ_3, IgG_3 ε, IgE. Number after hyphen refers to subclone number.

* Antibodies from these hybridomas immunoprecipitate natural breakdown products of M_r 45,000 and 34,000.

† +, Antibodies bound to both R-MuLV virus and R-MuLV-derived recombinant virus-coated microtiter plates; −, Antibodies bound only to R-MuLV-coated microtiter plates.

‡ Antibodies from these hybridomas immunoprecipitate natural breakdown products of M_r 45,000.

§ Antibodies from these hybridomas immunoprecipitate natural breakdown products of M_r 32,000.

Peptides present only in R-MuLV gp70 (closed circles, Fig. 3C) virtually all reside within the COOH-terminal P32 fragment (compare Fig. 3C to Fig. 2 D and F). Certain peptides (crosshatched, Fig. 3C) were present only in R-319 gp70. Some minor peptides that are not readily visible in the photographs were clearly present in the autoradiographs and are included in the composite.

Fig. 3 D and E shows fragments of M_r ≈45,000 generated by cleavage of R-MuLV and R-319 gp70s, respectively, with formic acid. Under these conditions, R-MuLV gp70 was cleaved to a fragment (Fig. 3D) that contained all the peptides common between P45 and P34, the P45-specific peptides, and two peptides normally in P32 (Fig. 2 D–F) that were absent from the recombinant R-319 (Fig. 3 B, C, and E). One P45-specific peptide was altered in mobility (arrow within circle) and the major P45/P34 shared peptides (open circles) were in common between R-MuLV gp70 and R-319 gp70. Thus, both hybridoma reactivities and peptide mapping indicate that the major differences between the parental ecotropic R-MuLV and the recombinant virus gp70s reside in the carboxyl half of P45 and the COOH-terminal P32 portion of the molecule. No differences were found between the gp70s of the XC⁻ ecotropic virus (R-240) and the dual tropic R-319 virus by either hybridoma reactivity or peptide analysis. The ramifications of these findings will be the subject of another report.

Tryptic peptide analyses have revealed a major peptide shared by the above recombinants and xenotropic viruses (2, 5, 10, 14). Fig. 4 shows the tryptic peptides of R-MuLV gp70 and R-319 gp70. Fig 4C shows a tryptic peptide pattern of a fragment with an apparent M_r of 32,000 derived by cleavage of R-319 gp70 with formic acid; note that the predominant feature is the xenotropic peptide (brackets). Common peptides between R-MuLV gp70 and R-319 are present along the baseline. Cleavage of FA32 derived from R-319 by using chymotrypsin (Fig. 4D) revealed the presence of the interspecies peptides (arrows, Fig. 3C) that characterize the COOH-terminal P32 portion of the molecule and are present in all gp70s tested (including primate and feline retrovirus gp70s). The other peptides are distinct from similarly derived peptides of R-MuLV gp70 (not shown).

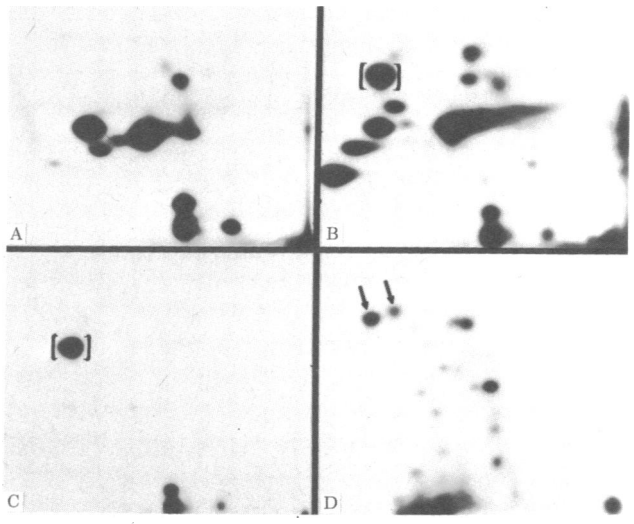

FIG. 4. Two-dimensional separation of tryptic peptides of R-MuLV gp70 and R-319 gp70. (A) Total R-MuLV gp70 digested by trypsin; (B) total R-319 gp70 digested by trypsin. Brackets denote peptide common to xenotropic and dual tropic virus gp70s and absent from ecotropic virus gp70s (note lack of this peptide in A). (C) Tryptic digest of a M_r 32,000 fragment of R-319 generated by treatment with formic acid. (D) Chymotryptic digest of formic acid-generated M_r 32,000 fragment of R-319 gp70. Double arrows denote peptides found in all gp70s (see Fig. 3) and which establish that FA32 is derived from the COOH terminus of R-319 gp70 by virtue of these structural markers (see Fig. 2 A and D–F).

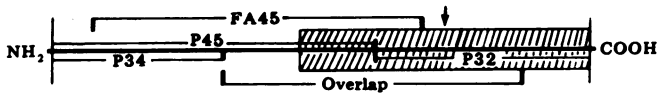

FIG. 5. Diagram of the relative domains of R-MuLV gp70 and orientation of acquired sequences. Relative locations of gp70 breakdown fragments are shown from the NH_2-terminus to the COOH terminus of gp70. Fragments are as defined in Figs. 1 and 2. Arrow denotes relative location of marker peptides common to all gp70s (see Figs. 3C and 4D). Crosshatched area indicates region of R-MuLV gp70 that is changed in the recombinants.

A diagram of the data described above is shown in Fig. 5. The relative locations of the fragments as well as the site of recombination are shown. The molecular sizes of the fragments are based on apparent molecular weights by $NaDodSO_4$/polyacrylamide electrophoresis and are overestimates due to the presence of glycosidic sidechains.

DISCUSSION

The natural breakdown of gp70 into discrete polypeptides of M_r 45,000 and 32,000 as well as several smaller fragments has been demonstrated previously (23). Because of the parallel breakdown of the two portions of the molecule into segments that had the same approximate electrophoretic mobility, it was not possible to interpret peptide maps of the total digest unambiguously (ref. 23 and our observations). Use of monoclonal antibodies allows the separation of fragments that are antigenically distinct, even though they have the same electrophoretic mobility. Mapping of the immunoprecipitated fragments clearly demonstrates them to be structurally distinct.

To date, most studies to localize the site of recombination have relied upon heteroduplex mapping (7, 25, 26) and oligonucleotide fingerprinting (3, 8, 27). The results of such studies have been remarkably consistent, indicating that the differences between the recombinant virus and the ecotropic parent lie in the 5′ half of the *env* gene. Because the 21S *env* message is twice as big as the gp70 molecule, it has not been possible to locate the site of recombination precisely. Reactivity patterns of monoclonal antibodies as well as peptide mapping of gp 70 breakdown products indicate that the major differences between the ecotropic parent and the recombinant viruses begin near the center of the gp70 molecule and extend through the COOH terminus. We leave open the possibility that the rest of the 3′ end of the genome has been replaced.

We cannot determine precisely the beginning of the recombination site because of ambiguity in assigning accurate molecular weights to the various gp70 fragments. The total molecule is 32% carbohydrate (28), and the mobilities of heavily glycosylated fragments are altered appreciably on $NaDodSO_4$/polyacrylamide gel electrophoresis. However, from other fragments generated by formic acid (which will cleave glycosidic side chains as well as aspartic acid-proline bonds), we estimate that the true molecular weights are approximately 40,000 for P45, 25,000 for P34, and 20,000 for P32. This would place the beginning of the recombination site in a region approximately 30,000 daltons from the NH_2 terminus of gp70.

Our data, in conjunction with nonhomologies demonstrated by heteroduplex analyses (7, 25, 26), suggest that gp70 terminates approximately 1700 bases from the 3′ end of the genome. DNA sequence data indicate that P15E resides between 887 and 1150 bases from the 3′ end (29). *In toto*, these data suggest that posttranslational processing may occur in the envelope precursor polyprotein between gp70 and p15E.

Our findings are consistent with previous conclusions that these *env* gene recombinants share determinants of xenotropic viruses (1–13). Moreover, the xenotropic virus relatedness is present in the COOH-terminal portion of the recombinant gp70. This finding supports our conclusion that R-MuLV gp70 and the derived recombinants share NH_2-terminal sequences and differ in the COOH-terminal portion of the molecule.

The authors gratefully acknowledge helpful discussions with and use of laboratory facilities provided by Dr. Richard Lerner. We also thank Dr. Marguerite Vogt for discussions and recombinant virus isolates used in this study. The advice and reagents provided by Drs. Norman Klinman, Judy Teale, Jeffery Hubert, David Katz, Thomas Shinnick, and Gregor Sutcliffe are also acknowledged. We thank Paula Eisenhart and Douglas Bingham for technical assistance. This research was supported in part by National Institutes of Health Grants CA 25803-02 and CA 25533-02, a Cancer Research Institute fellowship (J.H.E.), and National Institutes of Health Postdoctoral Fellowship NO1-F32-CA06233-01 (H.L.N.) and Training Grant 08-T32-GM0743702 (H.L.N.). This is publication no. 166 from the Department of Cellular and Developmental Immunology and no. 2100 from the Research Institute of Scripps Clinic.

1. Hartley, J. W., Wolford, M. K., Old, L. J. & Rowe, W. P. (1977) *Proc. Natl. Acad. Sci. USA* **74**, 789–792.
2. Elder, J. H., Gautsch, J. W., Jensen, F. C., Lerner, R. A., Hartley, J. W. & Rowe, W. P. (1977) *Proc. Natl. Acad. Sci. USA* **74**, 4676–4680.
3. Rommelaere, J., Faller, D. V. & Hopkins, N. (1978) *Proc. Natl. Acad. Sci. USA* **75**, 495–499.
4. Fischinger, P. J., Nomura, S. & Bolognesi, D. P. (1975) *Proc. Natl. Acad. Sci. USA* **72**, 5150–5154.
5. Fischinger, P. J., Frankel, A. E., Elder, J. H., Lerner, R. A., Ihle, J. N. & Bolognesi, D. P. (1978) *Virology* **90**, 241–254.
6. Van Griensven, L. J. L. D. & Vogt, M. (1980) *Virology* **101**, 376–388.
7. Chien, Y.-H., Verma, I. M., Shih, T. Y., Scolnick, E. M. & Davidson, N. (1978) *J. Virol.* **28**, 352–360.
8. Shih, T. Y., Wecks, M. O., Troxler, D. H., Coffin, J. M. & Scolnick, E. M. (1978) *J. Virol.* **26**, 71–83.
9. Vogt, M. (1979) *Virology* **93**, 226–236.
10. Elder, J. H., Jensen, F. C., Gautsch, J. W. & Lerner, R. A. (1978) in *Advances in Comparative Leukemia Research 1977*, eds. Bentvelzen, P., Hilgers, J. & Yohn, D. S. (Elsevier, Amsterdam), pp. 156–159.
11. Devare, S. G., Rapp, U. R., Todaro, G. J. & Stephenson, J. R. (1978) *J. Virol.* **28**, 457–465.
12. Troxler, D. H., Yuan, E., Linemeyer, D., Ruscetti, S. & Scolnick, E. M. (1978) *J. Exp. Med.* **148**, 639–653.
13. Troxler, D. H., Lowey, D., Howk, R., Young, H. & Scolnick, E. M. (1977) *Proc. Natl. Acad. Sci. USA* **74**, 4671–4675.
14. Elder, J. H., Jensen, F. C., Bryant, M. L. & Lerner, R. A. (1977) *Nature (London)* **267**, 23–28.
15. Strand, M. & August, J. T. (1973) *J. Biol. Chem.* **248**, 5627–5633.
16. Laemmli, U. K. (1970) *Nature (London)* **227**, 680–685.
17. Shulman, M., Wilde, C. D. & Kohler, G. (1978) *Nature (London)* **276**, 269–270.
18. Gefter, M. L., Margulies, D. H. & Scharff, M. D. (1977) *Somatic Cell Genet.* **3**, 231–236.
19. Pierce, S. K. & Klinman, N. R. (1977) *J. Exp. Med.* **146**, 509–519.
20. Nowinski, R. C., Lostrom, M. E., Tam, M. R., Stone, M. R. & Burnette, W. N. (1979) *Virology* **93**, 111–126.
21. Ternynck, T. & Avrameas, S. (1977) *Immunochemistry* **14**, 767–774.
22. Schaffhausen, B. S., Silver, J. E. & Benjamin, T. L. (1978) *Proc. Natl. Acad. Sci. USA* **75**, 79–83.
23. Krantz, M. J., Strand, M. & August, J. T. (1977) *J. Virol.* **22**, 804–815.
24. Henderson, L. E., Copeland, T. D., Smythers, G. W., Marquardt, H. & Oroszlan, S. (1978) *Virology* **85**, 319–322.
25. Donoghue, D. J., Rothenberg, E., Hopkins, N., Baltimore, D. & Sharp, P. A. (1978) *Cell* **14**, 959–970.
26. Bosselman, R. H., Van Griensven, L. J. L. D., Vogt, M. & Verma, I. M. (1979) *J. Virol.* **32**, 968–978.
27. Faller, D. V., Rommelaere, J. & Hopkins, N. (1978) *Proc. Natl. Acad. Sci. USA* **75**, 2964–2968.
28. Marquardt, H., Gilden, R. V. & Oroszlan, S. (1977) *Biochemistry* **16**, 710–717.
29. Sutcliffe, J. G., Shinnick, T. M., Verma, I. M. & Lerner, R. A. (1980) *Proc. Natl. Acad. Sci. USA* **77**, 3302–3306.